

Resonant spin polarization in a two-dimensional hole gas: Effect of the Luttinger term, structural inversion asymmetry and Zeeman splitting

Tianxing Ma*

*Max Planck Institute for the Physics of Complex Systems,
D-01187 Dresden, Germany*

The electric-field-induced resonant spin polarization of a two-dimensional hole gas described by Luttinger Hamiltonian with structural inversion asymmetry and Zeeman splitting in a perpendicular magnetic field was studied. The spin polarization arising from splitting between the light and the heavy hole bands shows a resonant peak at a certain magnetic field. Especially, the competition between the Luttinger term and the structural inversion asymmetry leads to a rich resonant peaks structure, and the required magnetic field for the resonance may be effectively reduced by enlarging the effective width of the quantum well. Furthermore, the Zeeman splitting tends to move the resonant spin polarization to a relative high magnetic field and destroy these rich resonant spin phenomena. Finally, both the height and the weight of the resonant peak increase as the temperature decreases. It is believed that such resonant spin phenomena can be verified in the sample of a two-dimensional hole gas, and it may provide an efficient way to control spin polarization by an external electric field.

PACS numbers: 73.43.-f,72.25.Dc,72.25.Hg,85.75.-d

INTRODUCTION

The physics of spin-orbit coupled system has attracted great attention in the field of spintronics. In particular, the spin-orbit coupling allows for manipulation of the electron spin via electric field, rather than magnetic field, creating the potential for applications in areas from spintronics to quantum computing[1, 2, 3]. Theoretically, the spin-orbit coupling reveals fundamental physics related to topological phases and their applications to the intrinsic and quantum spin Hall effect[4, 5, 6, 7, 8, 9]. Experimentally, electric-induced spin accumulation has been reported in an electron doped sample with the use of Kerr rotation microscopy[10, 11] and in a two-dimensional hole gas (2DHG) by angle-resolved polarization detection[12].

To identify the intrinsic spin Hall effect in experiments, resonant intrinsic spin Hall conductance has been predicted by several authors[13, 14, 15]. In a perpendicular magnetic field, the resonance effect in the two-dimensional electron gas (2DEG) stems from energy crossing of different Landau levels near the Fermi level due to the competition of Zeeman energy splitting and Rashba spin-orbit coupling[13], while in the hole-doped system, the resonant intrinsic spin Hall conductance is due to the transition between mostly spin- $-\frac{1}{2}$ holes and spin- $-\frac{3}{2}$ holes[14]. Even in the absence of a magnetic field, the Rashba term induces an energy level crossing in the lowest heavy hole subband, which gives rise to a resonant spin Hall conductance in a 2DHG[15]. However, there have not yet been experimental reports on the observation of the resonant spin Hall effect or related phenomena, which is likely due to the combination of the difficulty in detecting the spin current or spin accumulation

in the high magnetic field and the lack of experimental efforts in looking into these phenomena[16].

Spin polarization induced by electric fields or currents has been proposed in the spin-orbit coupled systems[17, 18, 19, 20], and several experiments have been devoted to generate spin polarization in semiconductors with spin-orbit coupling[21]. Very recently, electric-field induced resonant spin polarization was predicted in a 2DEG[20]. It was found that a tiny electric field may generate a finite spin polarization in a disordered Rashba system in the presence of a magnetic field. As a result, the electric spin susceptibility exhibits a resonant peak when the Fermi surface goes through the crossing point of two Landau levels, which provides a mechanism to control spin polarization efficiently by an electric field in semiconductors. As the spin polarization can be measured very accurately, it is believed that the effect can be verified in the samples of a 2DEG[20].

In this paper, we study the resonant electric-field-induced spin polarization of a 2DHG in detail, which has some intriguing and observable physical consequences. The general form to describe the spin transport in a 2DHG is the Luttinger model[22] with Rashba spin-orbit coupling arising from the structural inversion asymmetry (SIA)[14, 15, 23, 24], and such a system has recently been realized in several experimental studies[12, 25]. When a magnetic field is present, the most general Hamiltonian should involve spin Zeeman terms. However, the Landé g factor may reduce its absolute value, pass through *zero* or even change sign under a hydrostatic pressure[26, 27, 28], and electrical transport measurements under hydrostatic pressure have been performed in the limit of vanishing Landé g factor in previous experiments[26, 27, 28]. In the presence of a perpendicular magnetic field, we find that the spin polarization arising from splitting between the light and the heavy hole bands shows a resonant peak at a certain magnetic field. Especially, the competition

*txma@pks.mpg.de

between the Luttinger term and the Rashba spin-orbit coupling leads to a rich resonant peaks structure, and the required magnetic field for the resonance may be effectively reduced by enlarging the effective width of the quantum well. However, the Zeeman splitting tends to move such resonant spin polarization to a relative high magnetic field and destroy these rich resonant spin phenomena. Finally, both the height and the weight of the resonant peak increase as the temperature decreases, and the effect of disorder is discussed. As the spin polarization can be measured very accurately it is believed that this effect can be verified in the sample of a 2DHG, and it may provide an efficient way to control spin polarization by an external electric field[16, 20].

THEORETICAL FRAMEWORK

Our starting Hamiltonian for a 2DHG in a magnetic field $B\hat{z}$ is a sum of Luttinger, spin- $\vec{S}=\frac{3}{2}$ SIA and the Zeeman terms[14, 15, 22, 23, 24]:

$$H = \frac{1}{2m}(\gamma_1 + \frac{5}{2}\gamma_2)\Pi^2 - 2\frac{\gamma_2}{m}(\Pi \cdot S)^2 + \alpha(\vec{S} \times \Pi) \cdot \hat{z} - \kappa \frac{e\hbar}{mc} S \cdot B \quad (1)$$

where $\Pi = P - \frac{e}{c}A$ is the mechanical momentum, $e = -|e|$ is the electric charge for an electron, m is the bare electron mass, and α is the Rashba spin-orbit coupling. In addition, γ_1 and γ_2 are two dimensionless parameters modeling the effective mass and spin-orbit coupling around the Γ point, and κ is the effective g -factor. The confinement of the well in the z direction quantizes the momentum along this axis, which is approximated by the relation $\langle p_z \rangle = 0$, $\langle p_z^2 \rangle \approx (\pi\hbar/d)^2$ for a quantum well with thickness d [23].

We use the explicit matrix notation with $S = \frac{3}{2}$ eigenstates in the order $S_z = +\frac{3}{2}, +\frac{1}{2}, -\frac{1}{2}, -\frac{3}{2}$. By introducing the destruction operator [22] $a = \frac{1}{\sqrt{2m\hbar\omega}}(\Pi_x + i\Pi_y)$, and the creation operator $a^\dagger = \frac{1}{\sqrt{2m\hbar\omega}}(\Pi_x - i\Pi_y)$ to describe the Landau levels, Hamiltonian (1) can be rewritten as

$$H = \hbar\omega \begin{pmatrix} H_{11} & i\sqrt{3}\lambda a^\dagger & -\sqrt{3}\gamma_2 a^{+2} & 0 \\ -i\sqrt{3}\lambda a & H_{22} & 2i\lambda a^\dagger & -\sqrt{3}\gamma_2 a^{\dagger 2} \\ -\sqrt{3}\gamma_2 a^2 & -2i\lambda a & H_{33} & i\sqrt{3}\lambda a^\dagger \\ 0 & -\sqrt{3}\gamma_2 a^2 & -i\sqrt{3}\lambda a & H_{44} \end{pmatrix} \quad (2)$$

$$H_{NN} = [\gamma_1 - (-1)^N \gamma_2](a^\dagger a + \frac{1}{2}) + \frac{\beta}{2}[\gamma_1 + (-1)^N 2\gamma_2] - (\frac{5}{2} - N)\kappa$$

where $N=1, 2, 3, 4$, the dimensionless parameters $\lambda = \alpha m \sqrt{\frac{c}{2\hbar e B}}$, $\beta = \frac{\pi^2 \hbar}{d^2 m \omega}$ and the magnetic length $l_b = \sqrt{\frac{\hbar c}{eB}}$. The corresponding eigenvectors are expressed

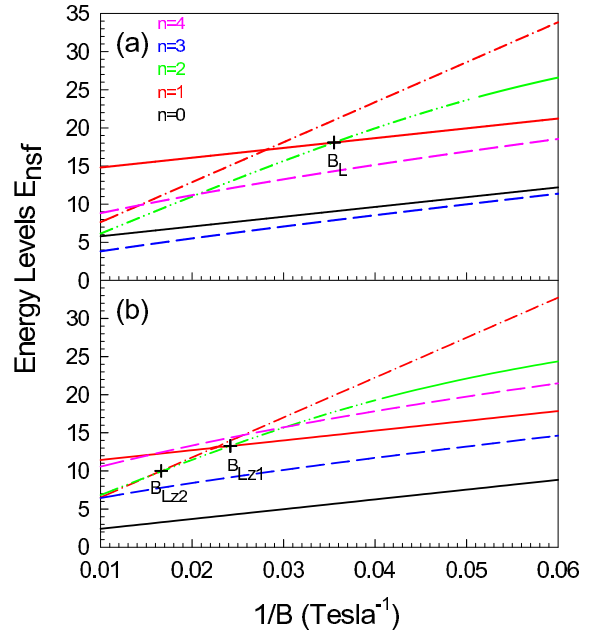


FIG. 1: (Color online) Landau levels (units: $\hbar\omega$) as functions of $1/B$. Different colors denote different n and only energy levels no higher than the energy level of resonant point are shown. Solid lines indicate Landau levels of mostly spin- $\frac{3}{2}$ holes, dashed lines indicate Landau levels of mostly spin- $\frac{1}{2}$ holes, dash-dot-dot lines indicate Landau levels of mostly spin- $\frac{1}{2}$ holes, dash-dot lines indicate Landau levels of mostly spin- $\frac{3}{2}$ holes. (a) $\kappa=0$; (b) $\kappa=2.25$.

as

$$|n, s, f\rangle = \begin{pmatrix} C_{nsf1}\phi_n \\ C_{nsf2}\phi_{n-1} \\ C_{nsf3}\phi_{n-2} \\ C_{nsf4}\phi_{n-3} \end{pmatrix}, \quad (3)$$

where ϕ_n is the eigenstate of the n th Landau level in the absence of the spin-orbit coupling, and n is a non-negative integer. In a large n limit, we can deduce that states $|n, +1, \pm 1\rangle$ indicate light-hole bands and $|n, -1, \pm 1\rangle$ indicate heavy-hole bands[14, 23]. We should add that when $n < 3$, the definition of $|n, s, f\rangle$ is not exact, so we simply take $|2, -1, 1\rangle$ as the lowest energy level of $n=2$ and $|1, 1, -1\rangle$ indicates the lowest energy level of $n=1$ in the whole paper.

If we apply a weak in-plane electric field in the y -direction, then the electric spin susceptibility can be evaluated by the Kubo formula in the linear response theory[29]

$$X_E^{\alpha y} = \frac{e\hbar}{L_x L_y} \mathbf{Im} \sum_{n's'f'} \frac{(f_{n's'f'} - f_{nsf})}{\epsilon_{nsf} - \epsilon_{n's'f'}} \times \frac{\langle n, s, f | S_\alpha | n', s', f' \rangle \langle n', s', f' | v_y | n, s, f \rangle}{\epsilon_{nsf} - \epsilon_{n's'f'} + i/\tau}, \quad (4)$$

$$f_{nsf} = \frac{1}{e^{(\epsilon_{nsf} - \mu)/k_B T} + 1},$$

where μ is the chemical potential, $\epsilon_{nsf} = \hbar\omega E_{nsf}$ is the eigenvalues within Eq. (1), and v_y is the velocity in y -direction. From the Kubo formula (4), we can see that only $n' = n \pm 1$ contributes to the spin susceptibility. In particular, it is natural to point out that if $\epsilon_{nsf} = \epsilon_{n \pm 1 s' f'}$ happens near the Fermi energy and for a long lifetime τ , a divergent $X_E^{\alpha y}$ may appear. Resonant spin phenomenon means an intriguing and observable physical consequence in experiments[14, 15, 16, 20, 30]. To be convenient for future experimental detection, we will discuss the effect of Luttinger term, SIA term, Zeeman splitting, and temperature on this resonant spin phenomenon in detail.

ENERGY LEVEL DEPENDING ON THE LUTTINGER TERM, STRUCTURAL INVERSION ASYMMETRY AND ZEEMAN SPLITTING

The properties of energy spectrum depending on magnetic field determine the behavior of spin transport. To further our story step by step, we study the energy levels as functions of the inverse of magnetic field within Eq. (1) when $\alpha=0$ firstly. Depending on the confinement scale d the Luttinger term is dominant for d not too small, while the SIA term becomes dominant for infinitely thin wells. Moreover, to learn the effect of Zeeman splitting on this resonant spin phenomenon, we distinguish Fig.1 (a) with $\kappa=0$ from Fig.1 (b) with $\kappa=2.25$ [22, 31]. Other parameters used are the same, $\gamma_1=6.92$, $\gamma_2=2.1$ and $d=8.3\text{nm}$ [12, 23].

We use lines with different colors to denote different n . In order to give a more clear illumination bellow, we only plot lines within energy levels no higher than the energy level of the resonant point, which shall contribute to the spin transport. As we have discussed, if the energy level crossing between states $|n, s, f\rangle$ and $|n \pm 1, s', f'\rangle$ occurs near Fermi energy, it may lead to a resonance. Though there are energy crosses that may lead to resonances when $1/B < 0.01 \text{ Tesla}^{-1}$ theoretically, the corresponding magnetic field is unavailable experimentally. Moreover, there are no energy cross when $1/B > 0.06 \text{ Tesla}^{-1}$ for present parameters, so we only consider the case when $0.01 \text{ Tesla}^{-1} < 1/B < 0.06 \text{ Tesla}^{-1}$.

In Fig.1 (a), the energy cross between states $|1, 1, -1\rangle$ and $|2, -1, 1\rangle$ occurs at $B_L=28.25 \text{ Tesla}$ (marked by a cross). For a set of sample's parameters, the behavior of energy levels depends on the magnetic field. Whether this energy cross shall lead to a resonance at the corresponding magnetic field, is determined by the hole density, which means that the "effective" energy cross shall appear near the Fermi energy, and this can be related directly to the filling factor, $\nu = \frac{N_h}{N_\phi} = \frac{n_h 2\pi\hbar c}{eB}$. As shown in Fig.1 (a), the realization of resonance requires that $3 < \frac{n_h 2\pi\hbar c}{eB_L} < 4$, and the hole density shall be $2.07 \times 10^{16}/\text{m}^2 < n_h < 2.75 \times 10^{16}/\text{m}^2$. Including

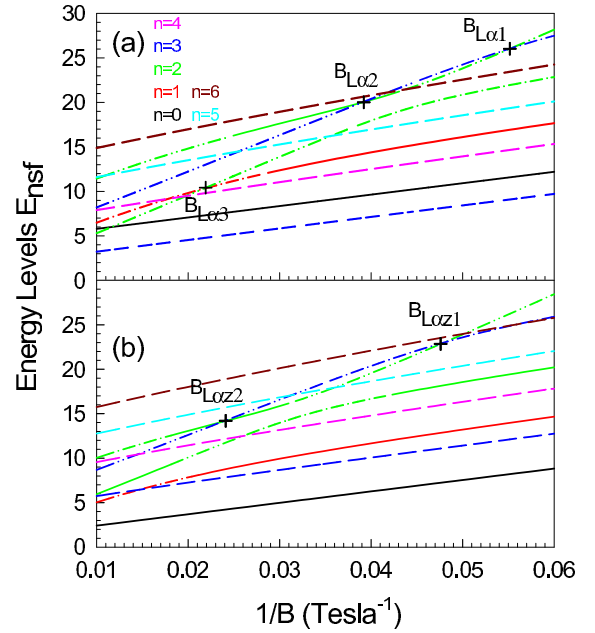


FIG. 2: (Color online) Caption is the same as that in Fig.1 except (a) $\alpha=10^5 \text{ m/s}$, and $\kappa=0$; (b) $\alpha=10^5 \text{ m/s}$, and $\kappa=2.25$.

the effect of Zeeman splitting, as shown in Fig.1 (b), the effective energy cross moves to a relative higher magnetic field, $B_{Lz1}=41.46 \text{ Tesla}$ (marked as a cross), and the required hole density for the resonance shall be $2 < \frac{n_h 2\pi\hbar c}{eB_{Lz1}} < 3$, i.e., $2.01 \times 10^{16}/\text{m}^2 < n_h < 3.01 \times 10^{16}/\text{m}^2$.

The energy cross occurring at B_{Lz1} means that $E_{1,1,-1}=E_{2,-1,1}$. When $\alpha=0$, an analytical equation can be derived from $E_{1,1,-1}=E_{2,-1,1}$, which is

$$B_{Lz1}d^2 = \frac{\pi^2\hbar c}{e} \frac{4\gamma_1\gamma_2 + 4\gamma_2^2}{\gamma_1^2 + 3\gamma_1\gamma_2 + 8\gamma_2^2 - 2\kappa(\gamma_1 + \gamma_2)}, \quad (5)$$

where we know that B_{Lz1} increases as κ increases. However, the Zeeman splitting introduce another resonant point at B_{Lz2} , which is due to the energy cross between sates $|1, 1, 1\rangle$ and $|2, -1, 1\rangle$, namely, $E_{1,1,1}=E_{2,-1,1}$. The required magnetic field

$$B_{Lz2}d^2 = \frac{\pi^2\hbar c}{e} \frac{4\gamma_2}{2\gamma_1 + 3\gamma_2 - \kappa - \frac{6\gamma_2^2}{\kappa}} \geq 0.853 \frac{\pi^2\hbar c}{e}, \quad (6)$$

and the equal sign is satisfied when $\kappa=\sqrt{6}\gamma_2$. The resonance at this point is introduced by the zeeman splitting since $\kappa=0$ is excluded from this equation. Moreover, B_{Lz2} is determined by the competition between the Luttinger term and the Zeeman splitting, and B_{Lz2} decreases as κ increases when $\kappa < \sqrt{6}\gamma_2$. From Eq. (5) and (6), it is useful to find that the required magnetic field for the resonance may be effectively reduced by enlarging the effective width of the quantum well.

Secondly, let us discuss the effect of SIA on this resonant spin phenomenon. The relatively large 5 meV measured spitting[12, 23] of the heavy hole band implies that

the effect of Rashba spin-orbit coupling arising from the SIA term is important. Energy levels as functions as $1/B$ with $\alpha=10^5\text{m/s}$ [12, 23] are shown in Fig.2, and we distinct (a) from (b) in case of $\kappa=0$ and $\kappa=2.25$. The key points that may lead to resonant spin transport have been marked as crosses in Fig. 2.

Comparing energy levels in Fig.1 (a) with those in Fig.2 (a), the SIA term moves the energy crosses (at $B_{L\alpha 3}$) between states $|1, 1, -1\rangle$ and $|2, -1, 1\rangle$ to a relative high magnetic field. However, a new set of energy crosses (at $B_{L\alpha 1}$ and $B_{L\alpha 2}$) appear in relative low magnetic fields, which are due to states $|2, 1, -1\rangle$ and $|3, -1, 1\rangle$, and there are at least three energy crosses which may lead to resonant spin transport. The first resonant point appears at $B_{L\alpha 1}=18.09$ Tesla, which requires that $7 < \frac{n_h^1 2\pi\hbar c}{eB_{L\alpha 1}} < 8$. The second resonant point appears at $B_{L\alpha 2}=25.70$ Tesla, requiring that $6 < \frac{n_h^2 2\pi\hbar c}{eB_{L\alpha 2}} < 7$. Since the properties of energy levels are depending on B through $\lambda=\alpha m\sqrt{\frac{c}{2\hbar e B}}$ and $\beta=\frac{\pi^2\hbar c}{d^2 e B}$, the new set of resonant points can be related to the competition between the SIA and the Luttinger term. It is interesting to point out that, if the range of n_h^1 and n_h^2 has some conjunct values, a rich resonant peaks structure of spin transport shall appear, and we will discuss this intriguing case bellow.

The energy levels as functions of $1/B$ when $\kappa=2.25$ have been shown in Fig. 2 (b). There are two effective energy crosses. However, the first resonant point appears at $B_{L\alpha z 2}=20.85$ Tesla, which requires that $7 < \frac{n_h^z 2\pi\hbar c}{eB_{L\alpha z 1}} < 8$, and the second resonant point appears at $B_{L\alpha z 2}=42.18$ Tesla, requiring $7 < \frac{n_h^z 2\pi\hbar c}{eB_{L\alpha z 2}} < 8$. The Zeeman splitting tends to move the resonant points to a higher magnetic field and resonance in a sample with a higher hole density is required.

Thirdly, to learn an overall understanding on the resonance depending of SIA term, we plot the required range of hole density for resonance as functions of α in Fig. 3 (a), and the magnetic field at resonant point as functions as α has been shown in the inset. These resonances are due to energy crosses of states $|2, 1, -1\rangle$ and $|3, -1, 1\rangle$, namely, $E_{2,1,-1}=E_{3,-1,1}$. The required range of hole density for resonance at the relative high magnetic field (range between dash dark lines) decreases as α increases. However, the required range of hole density for resonance at the relative low magnetic field (range between red lines) increases as κ increases, and there is a conjunct scope (gray area in Fig. 3 (a)), which shall lead to a rich resonant peaks structure for a sample by changing the magnetic field.

Let us take a look on energy levels in Fig.1 (a) and Fig.1 (b) together, as well as those in Fig.2 (a) and Fig.2 (b). It seems that larger effective g -factor κ will move such resonant spin transport to a higher magnetic field. To learn more on this aspect, we study the effect of κ on the required hole density for resonance, as well as magnetic field at resonant point. These resonances are

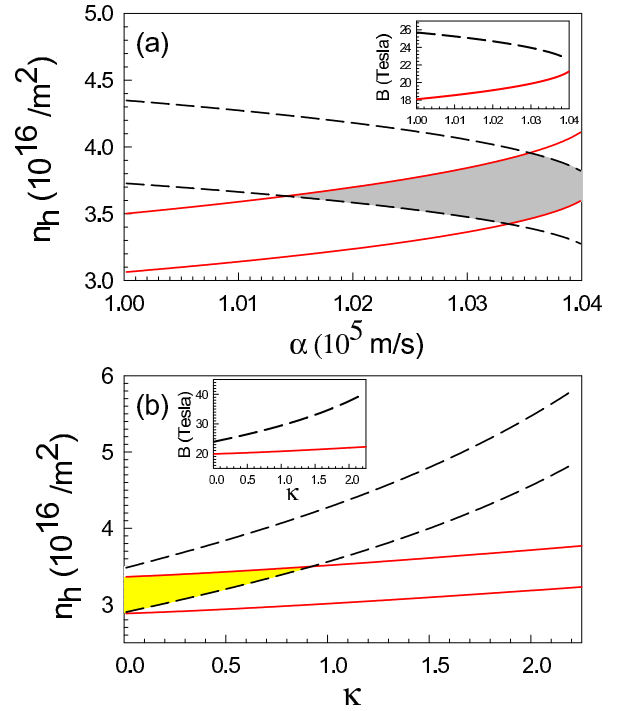


FIG. 3: (Color online) The required range of hole density for resonance at the relative high (area between dark dash lines) and low (area between red lines) magnetic field as functions of (a) α when $\kappa=0$; (b) κ at $\alpha=1.03 \times 10^5 / \text{m}^2$. Inset: magnetic fields at two different resonant points as function of (a) α when $\kappa=0$; (b) κ at $\alpha=1.03 \times 10^5 / \text{m}^2$.

due to energy crosses of states $|2, 1, -1\rangle$ and $|3, -1, 1\rangle$, and parameters used are $\gamma_1=6.92$, $\gamma_2=2.1$, $d=8.3\text{nm}$, and $\alpha=1.03 \times 10^5 \text{ m/s}$. As shown in Fig. 3 (b), the required range of hole density for resonance at the relative high magnetic field (range between dash dark lines) increases more quickly than the required range of hole density at the relative low magnetic field (range between red lines) as κ increases, which removes the conjunct scope (yellow area in Fig. 3 (b)), and the rich resonant spin transport of a sample will disappear as κ is large enough.

RESONANT SPIN SUSCEPTIBILITY

Now let us turn to study the resonant spin susceptibility. Our numerical result for X_E^{yy} has been shown in Fig.4 (a), and a remarkable rich resonant peaks structure appears, which indicate that a weak field may induce an intriguing and observable physical consequence of a 2DHG in the presence of a perpendicular magnetic field. Since the value of κ can be reduced by using hydrostatic pressure[26, 27, 28], we take $\kappa=0$ without loss of generality. Other parameters used are $n_h=3.6 \times 10^{16} / \text{m}^2$, $\gamma_1=6.92$, $\gamma_2=2.1$, $d=8.3\text{nm}$, and $\alpha=1.03 \times 10^5 \text{ m/s}$. The magnetic fields for resonances are respectively $B_{r1}=19.87$ Tesla, $B_{r2}=23.96$ Tesla, and $B_{r3}=46.42$ Tesla, which are

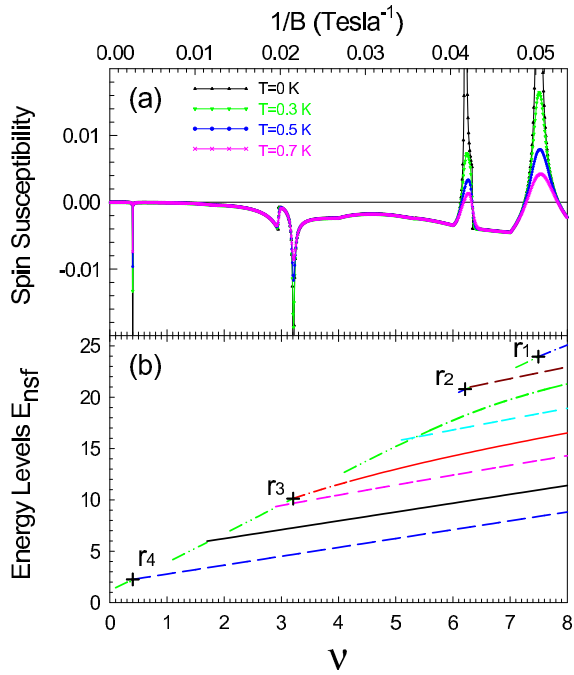


FIG. 4: (Color online) (a) Resonant spin susceptibility versus $1/B$ (or ν) at several temperatures for weak electric field. Parameters used are the same as those in Fig. 2 (a) except $\alpha=1.03 \times 10^5$ m/s. (b) Landau levels as functions of fill factors ν . Different colors denote different n and only energy levels occupied for corresponding ν are shown.

in the range of present experimental capability, and B_{r_4} is rather high so it need not be considered. Every energy cross for the resonance has been marked as r_1 , r_2 , r_3 and r_4 in Fig. 4 (b), and a careful analysis reveals that the resonance at r_1 and r_3 are contributed from the transition between mostly spin- $-\frac{1}{2}$ and mostly spin- $-\frac{1}{2}$ holes, and the resonance at r_2 is due to the interplay between mostly spin- $-\frac{1}{2}$ and mostly spin- $-\frac{3}{2}$ holes. As the spin polarization can be measured very accurately, it is believed that this effect can be verified in the samples of a 2DHG. Temperature is another important factor on this resonant spin polarization. In Fig. 4 (a), we have also plotted resonant spin susceptibility at several temperatures. As we can see, both the height and the width of the resonant peak increase as the temperature decreases at low temperature.

As we have discussed, the required magnetic field for the resonance may be effectively reduced by enlarging the effective width of the quantum well. To be convenient for future experimental detection, and learn more on the effect of temperature, we show resonant spin susceptibility at several temperatures for a relative low magnetic field in Fig. 5. The resonance appears at about 12.96 Tesla and the peak is still prominent even at 0.5 K. In the inset of Fig. 5, we show the temperature dependence of the height of the resonant peak. The characteristic temperature for the occurrence of the peak can be estimated to

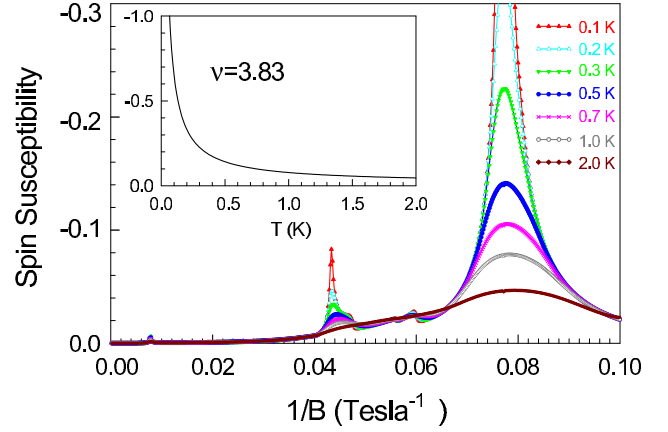


FIG. 5: (Color online) Resonant spin susceptibility (units: $\hbar/4\pi l_b^2 N/C$) versus $1/B$ at several temperature. The parameters are the same as those in Fig. 4 except $d = 13$ nm and $n_h=1.2 \times 10^{16}/\text{m}^2$. In the inset, temperature dependence of the height of the resonance peak is plotted.

be about 2 K at the resonant field for the parameters in the caption.

We have assumed no potential disorder in our theory. The effect of disorder in the 2DHG with spin-orbit coupling, especially in a strong magnetic field, is not well understood at this point[32, 33]. However, the effect of disorder on such kind of resonant spin phenomena in a 2DEG has been discussed by Bao and Shen[20] most recently. Their numerical simulation illustrated that impurity potential opens an energy gap near the resonant point and suppressed the effect gradually with increasing strength of disorder. Although the resonant spin phenomena in a 2DHG is much richer and more complicated, the essential nature of resonance is the same as the case in a 2DEG, which is caused by the energy crossing between different Landau levels. Moreover, in the absence of a magnetic field, numerical study of the spin transport in the Luttinger model indicates that the spin transport in the weak disorder regime remain almost the same as the value for the pure system[33]. It seems to be reasonable to assume that resonant spin polarization in a 2DHG shall survive in the weak disorder regime.

SUMMARY

In summary, we have studied the electric-field-induced resonant spin polarization of a 2DHG within the Luttinger model with structural inversion asymmetry and Zeeman splitting in a perpendicular magnetic field. The spin polarization arising from splitting between the light and the heavy hole bands shows a resonant peak at a certain magnetic field, and a rich resonant peaks structure is predicted, which is due to the competition between

the Luttinger term and the structural inversion asymmetry. The required magnetic field for the resonance may be effectively reduced by enlarging the effective width of the quantum well. However, the Zeeman splitting tends to move the resonant spin polarization to a relative high magnetic field and destroy this rich resonant peaks structure. Finally, the resonant value of the electric spin susceptibility decay with the temperature. Our calculations show that the parameters (the magnetic field, the effective g -factor, the hole density, the well thickness, and the Rashba spin-orbit coupling strength) for the resonance are likely accessible in experiments. It is believed that such resonant spin phenomena can be verified in the samples of two-dimensional hole gas, and it provides an efficient way to control spin polarization by an external electric field.

We thank Shun-Qing Shen for careful reading and many helpful discussions. We thank Yun-Juan Bao and Qin Liu for many helpful discussions.

-
- [1] S. A. Wolf, D. D. Awschalom, R. A. Buhrman, J. M. Daughton, S. von Molnar, M. L. Roukes, A. Y. Chtchelkanova, and D. M. Treger, *Science* **294**, 1488 (2001).
- [2] *Semiconductor Spintronics and Quantum Computation*, edited by D. D. Awschalom, D. Loss, and N. Samarth (Springer-Verlag, Berlin, 2002).
- [3] I. Zutic, J. Fabian, and S. Das Sarma, *Rev. Mod. Phys.* **76**, 323 (2004).
- [4] S. Murakami, N. Nagaosa, and S. C. Zhang, *Science* **301**, 1378 (2003).
- [5] J. Sinova, D. Culcer, Q. Niu, N. A. Sinitsyn, T. Jungwirth, and A. H. MacDonald, *Phys. Rev. Lett.* **92**, 126603 (2004).
- [6] C. L. Kane and E. J. Mele, *Phys. Rev. Lett.* **95**, 226801 (2005).
- [7] B. A. Bernevig and S. C. Zhang, *Phys. Rev. Lett.* **96**, 106802 (2006).
- [8] B. A. Bernevig, T. L. Hughes, and S. C. Zhang, *Science* **314**, 1757 (2006).
- [9] X. L. Qi, Y. Wu, and S. C. Zhang, *Phys. Rev. B* **74**, 085308 (2006).
- [10] Y. K. Kato, R. C. Myers, A. C. Gossard, D. D. Awschalom, *Science* **306**, 1910 (2004).
- [11] V. Sih, R. C. Myers, Y. K. Kato, W. H. Kato, W. H. Lau, A. C. Gossard, and D. D. Awschalom, *Nature (London), Phys. Sci.* **1**, 31 (2005).
- [12] J. Wunderlich, B. Kaestner, J. Sinova, and T. Jungwirth, *Phys. Rev. Lett.* **94**, 047204 (2005).
- [13] S. Q. Shen, M. Ma, X. C. Xie and F. C. Zhang, *Phys. Rev. Lett.* **92**, 256603 (2004); S. Q. Shen, Y. J. Bao, M. Ma, X. C. Xie and F. C. Zhang, *Phys. Rev. B* **71**, 155316 (2005).
- [14] Tianxing Ma, Qiu Liu, *Phys. Rev. B* **73**, 245315 (2006).
- [15] X. Dai, Z. Fang, Y. G. Yao, F. C. Zhang, *Phys. Rev. Lett.* **96**, 086802 (2006).
- [16] F. C. Zhang and S. Q. Shen, *cond-mat/0703176*.
- [17] V. M. Edelstein, *Solid State Commun.* **71**, 233 (1990); L. I. Magarill, A. V. Chaplik, and M. V. Entin, *Semiconductors* **35**, 1081 (2001).
- [18] J. i. Inoue, G. E. W. Bauer, and L. W. Molenkamp, *Phys. Rev. B* **67**, 033104 (2003).
- [19] X. Ma, L. Hu, R. Tao, and S. Q. Shen, *Phys. Rev. B* **70**, 195343 (2004); L. Hu, J. Gao, and S. Q. Shen, *Phys. Rev. B* **70**, 235323 (2004).
- [20] Y. J. Bao and S. Q. Shen, *Phys. Rev. B* **76**, 045313 (2007).
- [21] N. P. Stern, S. Ghosh, G. Xiang, M. Zhu, N. Samarth, and D. D. Awschalom, *Phys. Rev. Lett.* **97**, 126603 (2006); C. L. Yang, H. T. He, Lu Ding, L. J. Cui, Y. P. Zeng, J. N. Wang, and W. K. Ge, *Phys. Rev. Lett.* **96**, 186605 (2006).
- [22] J. M. Luttinger, *Phys. Rev.* **102**, 1030 (1956).
- [23] B. A. Bernevig and S. C. Zhang, *Phys. Rev. Lett.* **95**, 016801 (2005).
- [24] R. Winkler, *Phys. Rev. B* **62**, 4245 (4245); *ibid.*, **71**, 113307 (2005); G. M. Minkov, A. A. Sherstobitov, A. V. Germanenko, O. E. Rut, V. A. Larionova, B. N. Zvonkov, *Phys. Rev. B* **71**, 165312 (2005); Z. F. Jiang, R. D. Li, S. C. Zhang, W. M. Liu, *Phys. Rev. B* **72**, 045201 (2005).
- [25] B. Grbić, R. Leturcq, K. Ensslin, D. Reuter, and A. D. Wieck, *Appl. Phys. Lett.* **87**, 232108 (2005); O. Klochan, W. R. Clarke, R. Danneau, A. P. Micolich, L. H. Ho, A. R. Hamilton, K. Muraki, and Y. Hirayama, *Appl. Phys. Lett.* **89**, 092105 (2006).
- [26] N. G. Morawicz, K. W. J. Barnham, A. Briggs, C. T. Foxon, J. J. Harris, S. P. Najda, J. C. Portal and M. L. Williams, *Semicond. Sci. Technol.* **8**, 333 (1993).
- [27] D. R. Leadley, R. J. Nicholas, D. K. Maude, A. N. Utjuzh, J. C. Portal, J. J. Harris, and C. T. Foxon, *Phys. Rev. Lett.* **79**, 4246 (1997).
- [28] D. K. Maude, M. Potemski, J. C. Portal, M. Henini, L. Eaves, G. Hill, and M. A. Pate, *Phys. Rev. Lett.* **77**, 4604 (1996); Vladimir I. Fal'ko and S. V. Iordanskii, *Phys. Rev. Lett.* **84**, 127 (2000).
- [29] *Many-Particle Physics*, 3rd edition, G. Mahan, Kluwer, New York, 2000.
- [30] Tianxing Ma, Qin Liu, *Appl. Phys. Lett.* **89**, 112102 (2006).
- [31] R. Winkler, *Spin-Orbit Coupling Effects in Two-Dimensional Electron and Hole System* (Springer, New York, 2003).
- [32] S. Murakami, *Phys. Rev. B* **69**, 241202(R) (2004); J. Schliemann and D. Loss, *Phys. Rev. B* **69**, 165315 (2004).
- [33] W. Q. Chen, Z. Y. Weng, and D. N. Sheng, *Phys. Rev. Lett.* **95**, 086605 (2005).